2002MNRAS.329..605F

Mon. Not. R. Astron. Soc. **329,** 605–619 (2002)

Hubble Space Telescope Wide Field Planetary Camera 2 observations of hyperluminous infrared galaxies

D. Farrah,[1]★ A. Verma,[2] S. Oliver,[3] M. Rowan-Robinson[1] and R. McMahon[4]

[1]*Blackett Laboratory, Imperial College, Prince Consort Road, London SW7 2BW*
[2]*Max-Planck-Institut fur Extraterrestrische Physik, Postfach 1312, 85741 Garching, Germany*
[3]*Astronomy Centre, University of Sussex, Falmer, Brighton BN1 9QJ*
[4]*Institute of Astronomy, University of Cambridge, Madingley Road, Cambridge CB3 0HA*

Accepted 2001 September 25. Received 2001 September 25; in original form 2000 May 31

ABSTRACT

We present *Hubble Space Telescope* Wide Field Planetary Camera 2 *I*-band imaging for a sample of nine hyperluminous infrared galaxies (HLIRGs) spanning a redshift range $0.45 < z < 1.34$. Three of the sample have morphologies showing evidence for interactions and six are quasi-stellar objects (QSOs). Host galaxies in the QSOs are detected reliably out to $z \sim 0.8$. The detected QSO host galaxies have an elliptical morphology with scalelengths spanning $6.5 < r_e(\mathrm{kpc}) < 88$ and absolute *k*-corrected magnitudes spanning $-24.5 < M_I < -25.2$. There is no clear correlation between the infrared (IR) power source and the optical morphology. None of the sources in the sample, including F15307+3252, shows any evidence for gravitational lensing. We infer that the IR luminosities are thus real. Based on these results, and previous studies of HLIRGs, we conclude that this class of object is broadly consistent with being a simple extrapolation of the ULIRG population to higher luminosities; ULIRGs being mainly violently interacting systems powered by starbursts and/or active galactic nuclei. Only a small number of sources, the infrared luminosities of which exceed $10^{13}\,\mathrm{L}_\odot$, are intrinsically less luminous objects that have been boosted by gravitational lensing.

Key words: gravitational lensing – galaxies: active – quasars: general – galaxies: Seyfert – galaxies: starburst – infrared: galaxies.

1 INTRODUCTION

One of the most important results from the *Infrared Astronomical Satellite* (*IRAS*) all-sky surveys was the detection of a new class of galaxy where the bulk of the bolometric emission lies in the infrared range (Soifer et al. 1984; Sanders & Mirabel 1996). This population becomes the dominant extragalactic population at luminosities above $L_{\mathrm{IR}} > 10^{11}\,\mathrm{L}_\odot$. At the extreme upper end of the *IRAS* galaxy population lie the hyperluminous infrared galaxies (HLIRGs), those with $L_{\mathrm{IR}} > 10^{13.0}\,h_{65}^{-2}\,\mathrm{L}_\odot$ (Rowan-Robinson 2000). The first HLIRG to be found, P09104+4109, was identified by Kleinmann et al. (1988), with a far infrared luminosity of $1.5 \times 10^{13}\,h_{50}^{-2}\,\mathrm{L}_\odot$. In 1991, Rowan-Robinson et al. identified F10214+4724 with $z = 2.286$ and a far infrared luminosity of $3 \times 10^{14}\,h_{50}^{-2}\,\mathrm{L}_\odot$. Later observations of this object revealed a huge mass of molecular gas [$10^{11}\,h_{50}^{-2}\,\mathrm{M}_\odot$ (Brown & vanden Bout 1991; Solomon, Downes & Radford 1992)], a Seyfert emission spectrum (Elston et al. 1994), very high optical polarization (Lawrence et al. 1993), and strong evidence for lensing with a magnification of ~ 10 at infrared wavelengths (Broadhurst & Lehar 1995; Graham & Liu 1995; Serjeant et al. 1995; Eisenhardt et al. 1996; Green & Rowan-Robinson 1996). These objects appeared to presage an entirely new class of infrared galaxy.

There are currently ~ 50 sources positively identified as HLIRGs, of which 13 were identified in spectroscopic follow-up observations of sources discovered in far infrared or submillimetre surveys (Rowan-Robinson 2000). Two of those 13 infrared (IR)-selected HLIRGs have been found to be lensed. By projecting population densities from the *IRAS* Faint Source Survey (FSS) Rowan-Robinson (2000) estimates that there are between 100 and 200 HLIRGs with 60-μm flux > 200 mJy over the whole sky.

The source and trigger of the IR emission in HLIRGs is currently the subject of considerable debate. ULIRGs appear to be powered by starburst and/or quasar activity triggered by interactions (Leech et al. 1994; Clements et al. 1996), the HLIRGs may simply be the high-luminosity tail of the ULIRG population. Rowan-Robinson (2000) argues that the majority of the emission at rest wavelengths $> 50\,\mu\mathrm{m}$ in HLIRGs is caused by starburst activity, implying star formation rates $> 1000\,\mathrm{M}_\odot\,\mathrm{yr}^{-1}$. If the rest-frame far infrared and submillimetre emission from HLIRGs is caused by star formation,

★E-mail: d.farrah@ic.ac.uk

© 2002 RAS

© Royal Astronomical Society • Provided by the NASA Astrophysics Data System

2002MNRAS.329..605F

then the implied star formation rates would be the highest for any objects in the Universe. This would strongly suggest these galaxies are going through their maximal star formation periods, implying that they are very young galaxies. A third possibility is that if the IR emission arises via some other mechanism [e.g. a transient IR luminous phase in quasi-stellar object (QSO) evolution] then these galaxies may represent an entirely different class of object.

In this paper we examine the morphologies of HLIRGs, their host galaxies and immediate environments in an attempt to discern the nature and origins of their IR emission. We present a sample of hyperluminous infrared galaxies imaged with the Wide Field Planetary Camera 2 (WFPC2) on board the *Hubble Space Telescope (HST)*. Sample selection and observations, and data analysis are described in Sections 2 and 3. Results are presented in Section 4, including sample morphology, lensing properties and descriptions of individual sources. Discussion of these results can be found in Section 5 and conclusions can be found in Section 6.

Unless otherwise stated we have taken $H_0 = 65\,\mathrm{km\,s^{-1}\,Mpc^{-1}}$ and $\Omega_0 = 1.0$.

2 OBSERVATIONS

2.1 Sample

The nine objects in this sample all have a far infrared luminosity close to or exceeding $10^{13}\,\mathrm{L_\odot}$, which cannot be explained by non-thermal emission. The redshift range spans $z = 0.44-1.34$, with a mean redshift of $z = 0.9$. Of the objects in this sample, seven were identified purely by IR selection techniques.

Three of the sources, F10026+4949, F12509+3122 and F14218+3845 were discovered as part of a redshift survey of 3703 *IRAS* FSS objects to a flux limit of 200 mJy (Oliver et al. 1996). PG1148+549 and PG1634+706 are *IRAS*-detected PG QSOs with spectral energy distributions (SEDs) indicating an IR luminosity of $L_{\mathrm{IR}} > 10^{13}\,\mathrm{L_\odot}$. F00235+1024, LBQS1220+0939 and F12358+1807 were discovered as the result of a systematic programme of statistical optical identification being carried out with the APM machine (McMahon et al., in preparation). This project uses robust statistical estimators to identify *IRAS* sources, taking into account the *IRAS* error ellipse and optical magnitudes of all potential optical counterparts. LBQS1220+0939 and F12358+1807 are associated with known quasars with $m_B < 18.5$, i.e. 10 times less bright in the rest-frame ultraviolet (UV) than the PG quasars. F12358+1807 lies slightly below the $10^{13}\,\mathrm{L_\odot}$ limit but is a member of the broad absorption-line quasar class. BAL QSOs are believed to exhibit excess far-IR emission and F12358+1807 is the most luminous object in its class. F15307+3252 is an *IRAS* source (Cutri et al. 1994) that has an IR luminosity in excess of $10^{13}\,\mathrm{L_\odot}$.

The *Hubble Space Telescope* data were taken in cycle 6 between 1997 March and July using the WFPC2. The coordinates of each source were centred on the Planetary Camera charge-coupled device (CCD), selected for its superior pixel scale and full sampling of the point spread function (PSF) over the Wide Field Camera CCDs (0.046-arcsec pixel^{-1} as opposed to $\sim$0.1 arcsec pixel^{-1}). Exposures were taken using the F814W filter, which corresponds closely to the *I*-band filter in the Cousins system. Each observation consisted of one short exposure (100–600 s) to image the brightest parts of each object with minimal saturation of the detector, and two or three longer exposures (700–1600 s), taken both to image the fainter regions of each source and to facilitate the subtraction of cosmic rays.

3 DATA ANALYSIS

3.1 Data reduction

All data sets were calibrated on arrival with the best available reference files, using the IRAF task CALWP2, and combined into a single image using the IRAF task GCOMBINE. Statistical weights were assigned to different exposures based on their exposure times. The GCOMBINE rejection algorithm CCDCRREJ, which incorporates the Planetary Camera CCD characteristics, was used to remove cosmic rays by comparison between different exposures. Pixels flagged as saturated in the deeper exposures were replaced by their scaled unsaturated counterparts from one of the shallower exposures, with suitably modified statistical weights. Following these steps the sky background was subtracted and warm pixels were removed by linear interpolation from their immediate neighbours.

Photometric solutions were calculated using the SYNPHOT package from the STScI, which is consistent with the solutions given by Holtzman et al. (1995), and are given in the VEGAMAG system. For the QSOs in the sample that were saturated in the central regions PSF fitting photometry was performed to accurately measure the true source magnitudes. Corrections were made for detector gain (for these observations the gain was $7e^{-}DN^{-1}$) and aperture size. Absolute magnitudes (without a *k*-correction term) were derived using the expression

$$M = m - 25 - 5\log\{(2c/H_0)(1+z)[1-(1+z)^{-1/2}]\}. \qquad (1)$$

We estimate that our derived relative magnitudes have an associated photometric error of approximately 5 per cent. Prescriptions for converting magnitudes in the *HST* filter system (the 'flight' system) into more conventional filter systems depend in some way on the object colours. The F814W filter is a good match to the Cousins *I*-band filter, the conversion factor is very small (<0.05 mag) and depends only slightly on the object colour. As the colours of our sample are not known we have not applied a conversion factor and our magnitudes, although referred to as *I*-band magnitudes, remain in the WFPC2 flight filter system. The difference between these magnitudes and the equivalent Cousins *I*-band magnitudes is small (<0.1 mag) and thus comparisons can readily be made between the two systems. Fluxes in jansky were obtained by multiplying the flux in erg cm^{-2} s^{-1}Å^{-1} by the central wavelength of the F814W filter in angstroms and then dividing by the central frequency in hertz. As such they do not include any bandpass colour correction.

k-corrections for the F814W filter were computed using the spectral synthesis package PEGASE and the associated galaxy templates (Fioc & Rocca-Volmerange 1997). Previous studies (Surace et al. 1998) have shown that the optical emission from very luminous *IRAS* galaxies is dominated by emission from old stellar populations, rather than an unobscured starburst. We therefore used models for evolved stellar populations to calculate *k*-corrections. The galaxy template for a stellar population of age 10^9 yr was generated using a Rana & Basu (1992) initial mass function and a star formation law $\tau(t) = \nu g(t)$, where $g(t)$ is the gas fraction. Published values of *k*-corrections can vary markedly, especially for bluer filters (e.g. Poggianti 1997). We estimate that the error in our computed values owing to uncertainties in initial mass functions, star formation laws, the age of the system and the assumed source spectrum is approximately 0.2 mag at $z = 0.45$, rising to 0.45 mag at $z = 1.33$. No corrections have been made for reddening caused by dust extinction.

© Royal Astronomical Society • Provided by the NASA Astrophysics Data System

2002MNRAS.329..605F

3.2 The point spread function

Host galaxies can only be resolved in QSOs if light from the central bright source, and from the host galaxy, can be separated. The most convenient way to accomplish this is by fitting a point source template to the QSO; the template being established from a set of observations of stellar PSFs that are a good match in filter, colour and detector position to the targets. For the objects in this sample no additional observations were made of nearby stars, and no suitable observed PSFs were available in the *HST* PSF archive. Synthetic PSFs were therefore generated using the TINYTIM v5.0 software (Krist 1995), recently updated to include field-dependent effects such as astigmatism, coma and focus.

Ten times oversampled PSFs were generated. These PSFs were then shifted by non-integer pixel distances, rebinned to normal resolution and convolved with the PC pixel scattering function. The agreement between these synthetic PSFs and observed (stellar) PSFs is generally excellent within radii of $\sim$2 arcsec. Beyond this radius scattered light in the WFPC2 optics can have a significant effect, an effect that is not modelled by the TINYTIM software. The effect of any systematic uncertainties in the PSF have also not been examined, such effects are, however, likely to be extremely small.

The resulting PSFs were then centroided and normalized to the image via a reduced χ^2 fit. It was found that all the images were saturated in the central regions to varying extents, mostly confined to the central 3×3 pixels and never beyond the central 5×5 pixels. In all cases the centralmost possible pixels were used, avoiding those that were saturated or that lay in the diffraction spikes. This method allows the image and PSF to be registered to within $\sim$0.2 pixels (estimated by visual inspection), and also gives a starting value for the PSF normalization.

3.3 Profile fitting

In order to determine the morphology of the host galaxies in the sample, both de Vaucoleurs and exponential disc profiles were fitted to the surface brightness profiles of the host galaxies. The de Vaucoleurs profile is of the form

$$I(r) = I_0 \exp\{ -7.67[(r/r_e)^{1/4} - 1]\} \quad (2)$$

and the exponential disc profile is of the form:

$$I(r) = I_0 \exp[-(r/h)]. \quad (3)$$

One-dimensional surface brightness profiles of the sources were extracted by fitting annuli spaced at 1-pixel intervals, fixing the ellipticity (at $\epsilon = 0.1$), semimajor axis and position angle. The PSF profile together with either a radial de Vaucoleurs or disc profile were then fitted to the source surface brightness profile, treating the PSF normalization as a third free parameter. This helps to minimize as far as possible the systematic errors introduced by subtracting off a 'best-guess' PSF and fitting a galaxy profile to the remaining light distribution. Fitting was carried out using Levenberg–Marquardt least-squares minimization in order to robustly derive the best-fitting parameters. Two-dimensional isophote fitting, using the IRAF task ELLIPSE, was also used to investigate the ellipticities and position angles for each host by iteratively fitting isophotes of constant surface brightness.

In order to quantify whether a host galaxy was detected or not we imposed the condition that a PSF + galaxy to QSO fit must be better than a pure PSF fit to at least 95 per cent confidence, computed via an F test. We excluded pixels within the central 0.1 arcsec, as pixels within this radius tend to be highly undersampled and in some cases saturated. We also excluded all pixels beyond 2 arcsec because of light scattered within the WFPC2 optics.

4 RESULTS

Coordinates, redshifts and measured F814W magnitudes for the sources can be found in Table 1, together with the optical morphologies, IR luminosities and any previously cited best-fitting IR SED models. Table 2 summarizes the host galaxy properties,

Table 1. Hyperluminous galaxies observed by *HST*.

Name	RA (2000)	Dec	z	f_{814}[a]	m_I	M_I[b]	L_{IR}[c]	IR SED[f]	Opt Spec.[g]	Morphology
F00235+1024	00 26 06.7	10 41 27.6	0.58	0.08	18.73	−23.6	13.1[d]	63 per cent Sb, 37 per cent AGN[d]	NL	Interacting
F10026+4949	10 05 52.5	49 34 47.8	1.12	0.04	19.61	−24.3	13.8[e]	AGN-dominated[e]	Sy1	Interacting
PG1148+549	11 51 20.4	54 37 32.8	0.97	2.07	15.21	−28.3	13.7	30 per cent Sb, 70 per cent AGN	QSO	Undisturbed
LBQS1220+0939	12 23 17.9	09 23 07.3	0.68	0.43	16.91	−25.8	13.5[e]	–	QSO	Undisturbed
F12358+1807	12 38 20.2	17 50 38.8	0.45	1.09	15.90	−25.9	12.7	–	BAL QSO	Undisturbed
F12509+3122	12 53 17.6	31 05 50.5	0.78	0.91	16.10	−26.9	13.5[e]	AGN-dominated[e]	QSO	Undisturbed
F14218+3845	14 23 55.5	38 31 51.3	1.21	0.07	18.96	−25.1	13.1[d]	74 per cent Sb, 26 per cent AGN[d]	QSO	Undisturbed
F15307+3252	15 32 44.1	32 42 46.2	0.93	0.14	18.20	−25.2	13.5[d]	32 per cent Sb, 68 per cent AGN[d]	Sy2	Interacting
PG1634+706	16 34 28.8	70 31 32.8	1.33	6.30	14.00	−30.4	14.0	17 per cent Sb, 83 per cent AGN	QSO	Undisturbed

Coordinates and absolute *F814W*-band magnitudes/fluxes are taken from the *HST* images and are in the VEGAMAG *HST* flight filter system.
[a] I-band flux in units of mJy. Subscript denotes wavelength in microns.
[b] No applied k-correction.
[c] Logarithm of the 1–1000 μm IR luminosity, where necessary recomputed for $H_0 = 65\,\mathrm{km\,s^{-1}\,Mpc^{-1}}$ and $\Omega_0 = 1.0$, and in units of bolometric solar luminosities.
[d] Verma et al. (2001).
[e] Rowan-Robinson (2000).
[f] IR spectral energy distribution, computed between 1 and 1000 μm.
[g] Optical spectral classification, taken from Rowan-Robinson (2000).

© Royal Astronomical Society • Provided by the NASA Astrophysics Data System

2002MNRAS.329..605F

Table 2. Host galaxy properties.

Galaxy	m_I	k^a	M_I^b	r_e (kpc)	I_e
F00235+1024	–	−1.18	−24.7	–	–
F10026+4949	–	−1.25	−25.5	6.7 ± 0.8	20.6 ± 0.16
1220+0939	19.0	−1.27	−25.0	87.9 ± 8.0	24.8 ± 0.15
F12358+1807	18.3	−0.94	−24.5	7.1 ± 0.29	20.8 ± 0.1
F12509+3122	19.1	−1.34	−25.2	10.3 ± 0.67	21.0 ± 0.13
F14218+3845	20.5	−1.10	−24.7	–	–
F15307+3252	–	−1.37	−26.4	12.4 ± 0.55	21.1 ± 0.79

F00235+1024, F10026+4949 and F15307+3252 are included here for completeness, in these cases the 'host' is in fact the source itself. All reliably determined profiles were ellipticals. Although a host for F14218+3845 was resolved the profile was undetermined. The morphology of F00235+1024 is too disturbed to fit a profile to. 2σ errors are quoted.

[a] k-correction for the F814W filter.

[b] Absolute magnitudes including k-corrections.

and includes relative/absolute magnitudes, k-corrections and host galaxy properties derived from profile fitting. In the sections where host galaxies are discussed, this refers to those objects listed in Table 2, thus including three sources that do not possess a central bright source. Discussion of PSF subtraction and/or host galaxy detection limits are not applicable to these objects.

4.1 Morphologies and lensing

The *HST* images showing the sources and immediate environments can be found in Fig. 1. Detailed images of each object can be found in Fig. 2.

The *HST* images show that the sample contains an interesting mixture of morphologies. Two of the sources, F00235+1024 and F15307+3252 show clear signs of strong interaction, features include obvious morphological disturbance, tails and compact bright 'knots'. One further source, F10026+4949 is small, shows

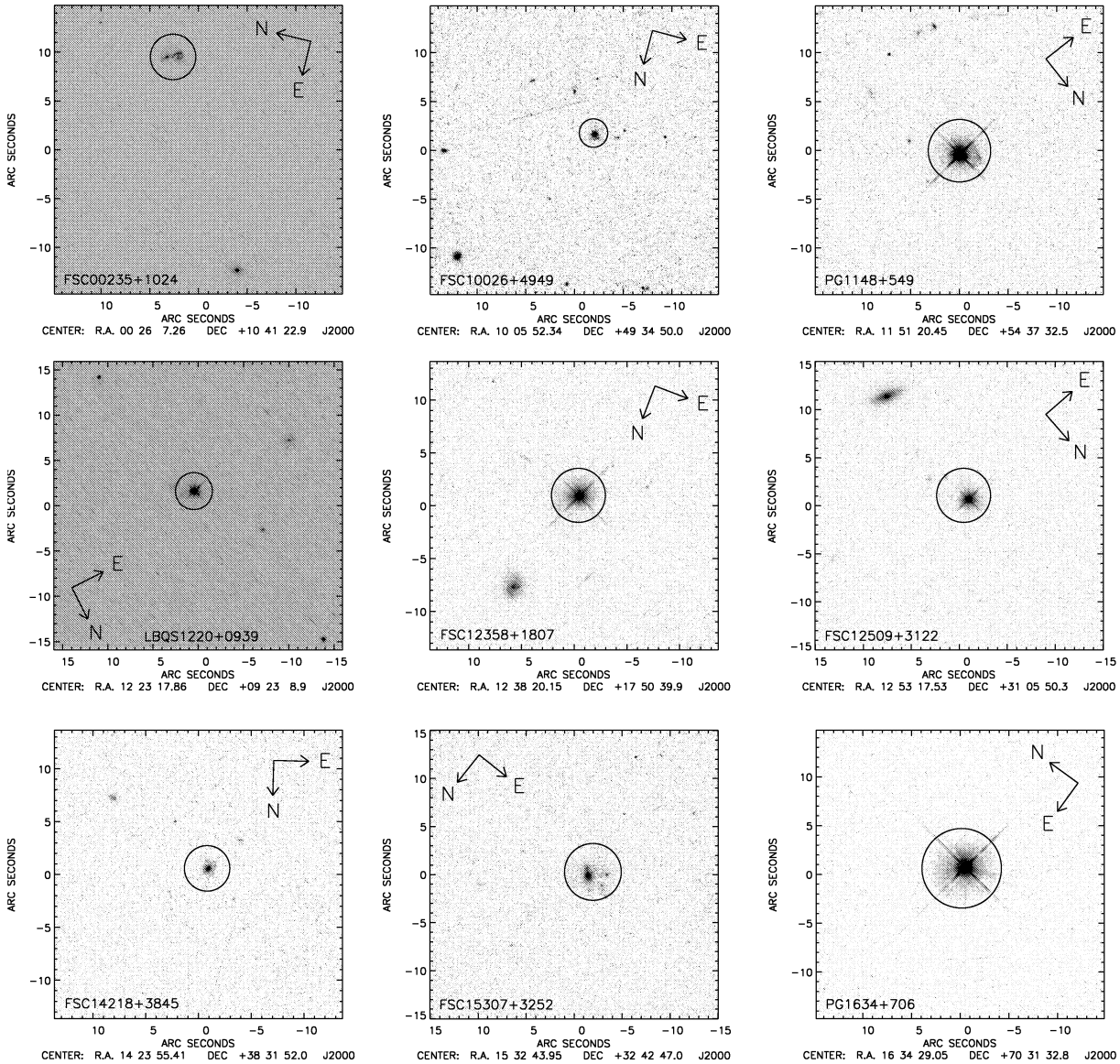

Figure 1. *HST* F814W-band images of the nine hyperluminous galaxies, showing the sources (circled) and immediate environments.

© Royal Astronomical Society • Provided by the NASA Astrophysics Data System

2002MNRAS.329..605F

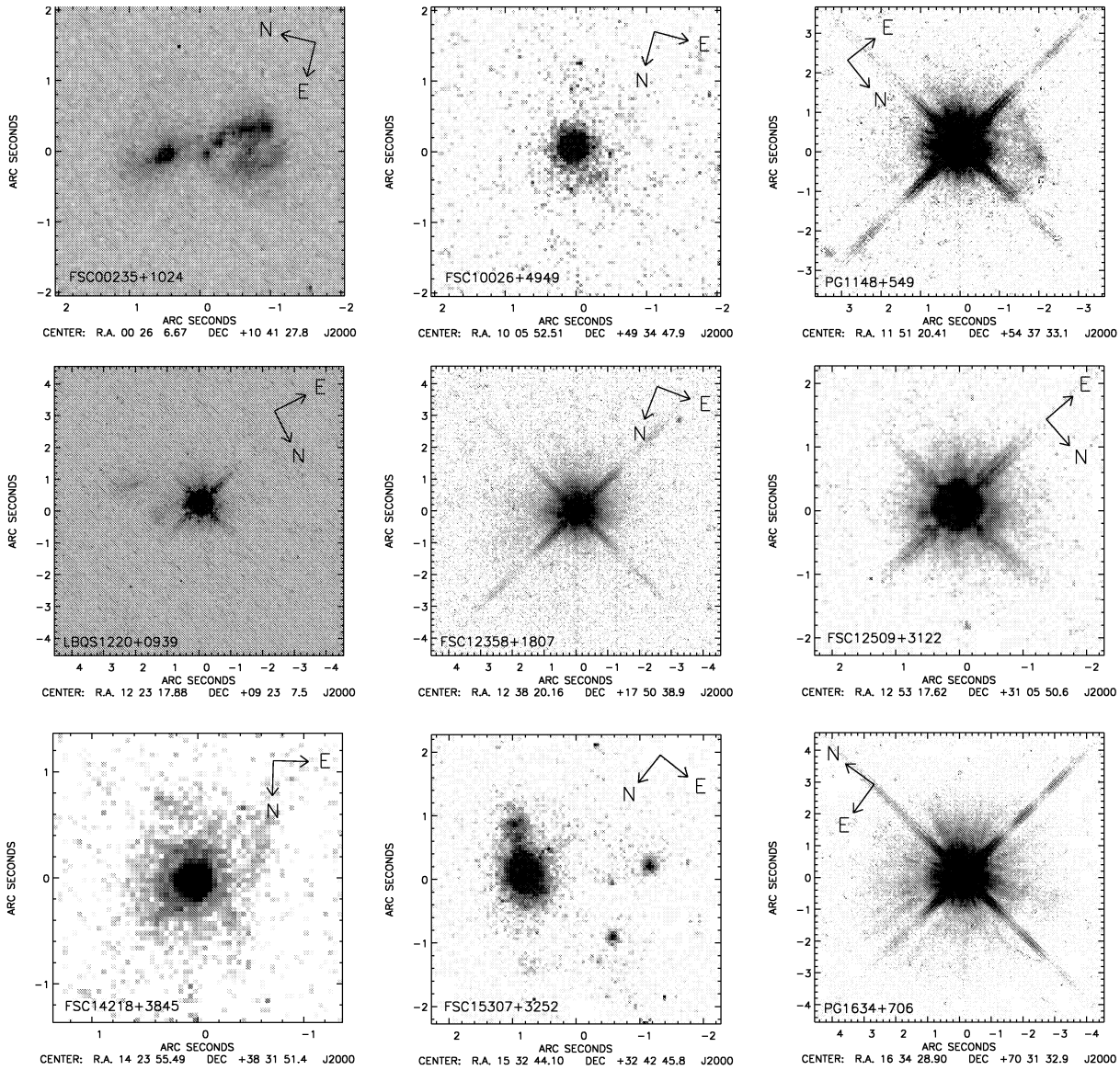

Figure 2. *HST* F814W images of the nine HLIRGs, showing the details of each source and scaled to show any interesting features.

no bright central source and slightly weaker signs of interaction. One object, F14218+3845, is a QSO with a relatively underluminous point source. The five remaining sources are all optically luminous QSOs. Although some of the QSOs show some very faint inhomogeneities, none of them show any definite signs of recent or ongoing interaction.

None of the objects in the sample show any evidence for gravitational lensing. We investigated the possibility of lensing for all sources using the *HST* gravitational lens simulator constructed by Kavan Ratnatunga as part of the *HST* Medium Deep Survey (Griffiths et al. 1994; Ratnatunga, Griffiths & Ostrander 1999). For non-trivial magnification, arcs of length comparable to the Einstein radius should be observed, so to first order we can set limits on the Einstein radius of 0.3 arcsec ($\sim$6 PC pixels). If any lensing is therefore present it would have to be by low-mass galaxies and so would make no appreciable difference to the derived optical and IR fluxes, unless the background source happened to be aligned with a caustic. The lack of multiple images around any of the QSOs limits any possible lensing magnification to less than a factor of 2 in these objects, assuming an isothermal sphere model. If no other signs of lensing are apparent at *HST* resolution, however, such as tangential stretching, then it is extremely unlikely that lensing contributes significantly to the luminosity of any of the objects in the sample. Those sources of which the morphologies are, on first impressions, plausibly consistent with some form of lensing scenario are discussed further in Section 4.5.

For two of the three sources not dominated by a bright point source, F10026+4949 and F15307+3252, we were able to fit theoretical galaxy surface brightness profiles. For both of these sources the galaxies were found to be extremely luminous ellipticals, the properties of which can be found in Table 2. The morphology of F00235+1024 is so disturbed that no type of galaxy profile can be fitted to the source surface brightness profile.

For the two PG quasars Schmidt & Green (1983) have measured fluxes at 440 nm. Their results, compared with the measured F814W fluxes given in Table 1, suggest that the optical continuum for both of these sources is extremely flat, with $\alpha \sim 0$.

© Royal Astronomical Society • Provided by the NASA Astrophysics Data System

2002MNRAS.329..605F

4.2 Infrared properties

Table 1 lists the IR properties of the sample. Three of the sources (F00235+1024, F14218+3845 and F15307+3252) have been observed previously by the *Infrared Space Observatory* (*ISO*) as part of a larger sample, and their spectral energy distributions modelled using a suite of active galactic nuclei (AGN) and starburst models (Verma et al. 2001). The IR emission from PG1634+706 has been modelled previously by Haas et al. (1998) using a series of greybody functions. The IR emission from a further three sources (F10026+4949, F12509+3122 and PG1148+549) has been examined previously by Rowan-Robinson (2000). For the final two sources in the sample (LBQS1220+0939 and F12358+1807) there exists insufficient photometry to model the power source behind the IR SED. Some constraints on the IR emission from F10026+4949 and F12509+3122 can also be drawn using the *IRAS* colours. A 'warm' infrared colour (i.e. when the *IRAS* 25- to 60-μm flux ratio has a value of $f_{25}/f_{60} \geq 0.2$) generally indicates the presence of an AGN (de Grijp et al. 1985). Both F10026+4949 ($f_{25}/f_{60} = 0.665$) and F12509+3122 ($f_{25}/f_{60} = 0.472$) possess 'warm' colours, and have been cited previously as containing an AGN by Rowan-Robinson (2000). For F12358+1807 and LBQS1220+0939 the *IRAS* fluxes and upper limits do not allow us to distinguish between 'warm' and 'cool' IR colours, hence the power source is unconstrained.

For two of the sources in the sample (PG1148+549 and PG1634+706) we present new fits to the IR SED. To study the IR emission from these two sources, we have fitted the SEDs using combinations of the following two models.

(i) The inclined AGN dust torus model (Efstathiou, private communication) is based on previous AGN models (Efstathiou, Hough & Young 1995; Efstathiou & Rowan-Robinson 1995). The model contains 15 different line-of-sight orientations, with a torus opening angle of 60° and a UV optical depth of $\tau_{\rm UV} = 1000$.

(ii) The pure starburst model (Efstathiou, Rowan-Robinson & Siebenmorgen 2000) is based on an ensemble of H II regions including an evolving population of young stars. It includes a simple model for the evolution of H II regions, and a dust grain model incorporating Polycyclic Aromatic Hydrocarbons (Siebenmorgen & Kruegel 1992). The set of models used have a star formation rate exponentially decaying at a fixed rate ($\tau = 20$ Myr), but with varying initial UV optical depth (four discrete values) and starburst lifetime (seven discrete values).

For PG1148+549 we have compiled additional IR photometry to that used in Rowan-Robinson (2000). We compiled the SED using *IRAS* fluxes, together with photometry from EUV spectra (Tripp, Bechtold & Green 1994). The *I*-band flux measured in this paper is in good agreement with this *EUVE* photometry. PG1634+706, although previously modelled in the IR using a suite of greybodies, has not been previously modelled using the latest generation of radiative transfer codes. For PG1634+706 the FIR emission has been well sampled by *ISO* (Haas et al. 1998), and we also include the *IRAS* fluxes. For both sources we also use the *I*-band fluxes taken from the *HST* images in this paper.

To fit the SEDs we have used the two models described above, allowing each model to vary freely in normalization. The starburst model is also allowed to vary in the discrete values of initial UV optical depth and starburst age. The torus model is also allowed to vary in inclination angle. The two models are then added together, and the reduced χ^2 estimator is calculated for the total of every combination of starburst plus AGN model. The best-fitting model is then selected using the minimum χ^2. The SEDs and best model fits for these two sources can be found in Fig. 3.

For PG1148+549 the fit to the IR SED is excellent. For PG1634+706 the fit is again very good, except that it underpredicts the *I*-band flux and very slightly overpredicts the FIR emission. The small inconsistencies in the far-IR are likely to be the result of having only a small number of input models with discrete parameter values, which do not sample the full parameter space of either the starburst or AGN models. The underprediction of the *I*-band flux in the SED is most probably also caused by this, but could also be accounted for by an unquantified contribution from evolved stellar populations that are not included in either model.

4.3 Companion sources

An L^* galaxy at the highest redshift in our sample ($z = 1.33$) would have a magnitude of approximately $m_I = 22.2$, and the faintest galaxies visible (to a 3σ detection) in any of our observations have a magnitude of $m_I \sim 22.5$. Companion sources, if present, should certainly be visible for all the sources in the sample.

Eight of the nine objects in the sample show at least one other

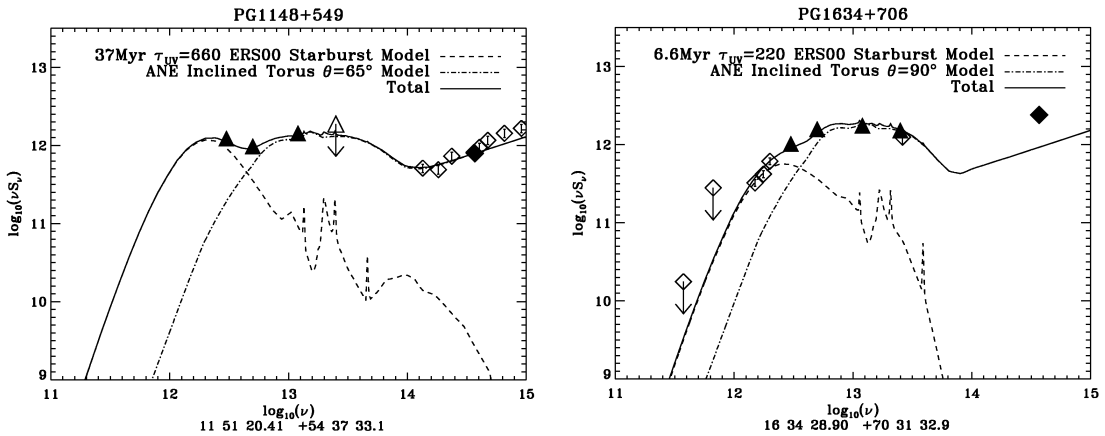

Figure 3. IR spectral energy distributions for PG1148+549 and PG1634+706. The filled triangles are *IRAS* fluxes, and the unfilled triangles with an arrow below them are *IRAS* upper limits. Filled diamonds are the *I*-band fluxes from this paper. Unfilled diamonds are any additional data taken from the literature. For PG1148+549 the additional data are taken from Tripp et al. (1994). For PG1634+706 the additional data are taken from Haas et al. (1998).

© Royal Astronomical Society • Provided by the NASA Astrophysics Data System

2002MNRAS.329..605F

object within the PC field of view. Two objects, F12358+1807 and F12509+3122 show a single large, bright companion, where the magnitude and the separation from the source plausibly suggest a cluster environment. F12358+1807 also has a number of smaller, dimmer companions. The other six objects all show at least two small, dim objects within 15 arcsec. For PG1634+706 there appear to be no other sources visible within the PC field of view. At the redshift of this source ($z = 1.33$), this would mean that there are no companions with an optical luminosity comparable to or brighter than L^* within 0.5 Mpc, suggesting that this source is isolated.

4.4 QSO host galaxy properties

Six objects in our sample are QSOs as determined from the optical morphologies, and host galaxies are clearly resolved in four of these six objects. Images of the four host galaxies can be found in Fig. 4. For a positive host galaxy detection our original imposition of a minimum 95 per cent confidence limit was found to be easily satisfied, with all detections achieving at least a 97.5 per cent confidence and two exceeding 99 per cent confidence. For the two PG quasars a combination of distance and extremely luminous central point source meant that the host was unresolved. The average value of the QSO host galaxy magnitude was found to be

$$\langle M_I \rangle = -24.9 \pm 0.4 \quad (4)$$

which is comparable in value to the magnitudes of the brightest cluster elliptical galaxies found in the Virgo and Coma clusters (Caon, Capaccioli & D'Onofrio 1994; Jorgensen & Franx 1994). It is also approximately 1.7-mag brighter than the field galaxy magnitude, $M_I^* = -23.2$ (Pozzetti, Bruzual & Zamorani 1996; Efstathiou, Ellis & Peterson 1988). For comparison the three objects that do not possess a bright central source are, on average, ~0.5-mag brighter than the mean QSO host galaxy magnitude, with $\langle M_I \rangle = -25.5 \pm 0.9$.

For three of the four QSOs in which a host was detected, the residual light profile was sufficiently bright and extended to allow a galaxy profile to be reliably fitted. All three hosts were found to be very luminous ellipticals, with large derived scalelengths. These values can be found in Table 2. The scalelength for LBQS1220+0939, at ~88 kpc is extremely large, and is comparable to the largest observed ellipticals. Measured ellipticities were found to be very small, generally $0.1 < \epsilon < 0.2$, justifying our use of a fixed ellipticity in extracting surface brightness profiles.

4.5 Individual sources

4.5.1 F00235+1024

$z = 0.58$. There is no X-ray detection down to a limit of $L_x/L_{\rm bol} = 2.3 \times 10^{-4}$, indicating either atypically weak X-ray emission or an obscuring column density of $N_{\rm H} > 10^{23}\,{\rm cm}^{-2}$ (Wilman et al. 1998). The IR power source is predominantly of starburst origin, but with a significant (37 per cent) AGN contribution (Verma et al. 2001).

The *HST* image shows an object that is clearly strongly interacting. There is a compact, bright region to the north, with traces of nebulosity extending further to the north. To the south the emission is less bright, more extended and shows some small plumes. Present throughout this region is a series of very compact,

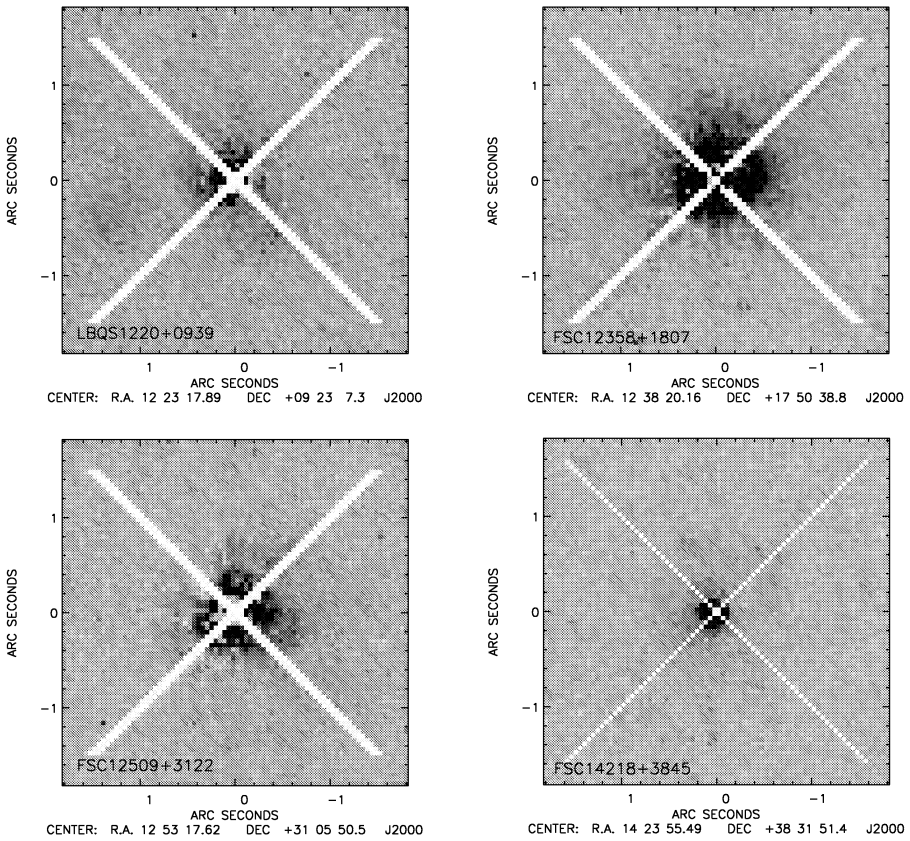

Figure 4. *HST* F814W images of the four resolved HLIRG QSO host galaxies. Residual PSF features have been masked out.

© Royal Astronomical Society • Provided by the NASA Astrophysics Data System

2002MNRAS.329..605F

bright, 'knots'. There are two small companion sources; one 6.9 arcsec to the north and one 23 arcsec to the east.

4.5.2 *F10026 + 4949*

$z = 1.12$. The IR power source of this object is best explained as being AGN-dominated, but with an uncertain starburst contribution (Rowan-Robinson 2000). The 'warm' IR colour ($f_{25}/f_{60} = 0.665$) also implies AGN dominance. The object is small (less than 1 arcsec in diameter), has a very low ellipticity (~ 0.1) and has no bright central source. There is some morphological disturbance in the form of faint nebulosity extending towards the east. Six small, dim companion sources are visible within a 6-arcsec radius, two of which lie within 3 arcsec. These very close companions and asymmetric light distribution imply recent or ongoing interactions. The surface brightness profile is best fitted by an elliptical profile, with $M_I = -25.5$ and a scalelength of 6.7 kpc.

4.5.3 *PG1148+549*

$z = 0.97$. This radio-quiet QSO is cited (Hamann et al. 1995) as probably containing the broad emission line Ne VIII. This would require a total column of $N_{\rm H} > 10^{22}$ cm^{-2}, and at least 33 per cent obscuration of the central regions. The presence of this line would mean that gas in the broad emission-line regions would be extremely hot, and that this component would appear as an X-ray warm absorber if it lies along the line of sight to the X-ray continuum source. Long-term broad-band optical photometry of this object (Barbieri et al. 1988) shows possible evidence for a variable source, with suspicious small-amplitude variability in the period 1968–1986.

The *HST* image shows a bright QSO with some faint nebulosity extending approximately 2.2 arcsec to the north-east. Three companion sources can be seen 4.3 arcsec to the south-west, 12.2 arcsec to the south and 13.2 arcsec to the south-east. A host galaxy was detected at greater than 97.5 per cent confidence, however, fitting a galaxy profile to the underlying light profile proved impossible. The measured host magnitude was also extremely large, at $M_I = -27.3$. It is therefore more likely that we are merely detecting a profile of light from the AGN that has been scattered within the host galaxy, rather than the host galaxy itself, hence the host is unresolved. The IR SED is best fitted by an AGN (70 per cent) at 65° line-of-sight orientation, and a 37-Myr starburst (30 per cent) with $\tau_{\rm UV} = 660$. The fit shows that the torus dominates the emission from 60 μm to the UV. The starburst dominates the emission longward of 60 μm. The orientation of the AGN model implies that the broad-line regions should be visible in the optical, which is consistent with the optical morphology.

4.5.4 *LBQS1220+0939*

$z = 0.68$. This very compact QSO possesses largely symmetrical, dim, extended nebulosity and appears to be morphologically undisturbed, except for some faint inhomogeneities to the south-west. There is a very dim companion source 2.1 arcsec to the south-west and two brighter companions <11 arcsec to the north-east. A PSF + host galaxy fit is preferred to a pure PSF fit at >99 per cent confidence, with an elliptical being strongly preferred to a spiral. The host galaxy has $M_I = -25.0$, and a scalelength of ~ 88 kpc. The average ellipticity of the source is 0.2. There is a gradient of decreasing ellipticity from the central regions ($\langle\epsilon\rangle = 0.1$ at 0.25 arcsec) to the outer regions ($\langle\epsilon\rangle = 0.3$ at 0.80 arcsec). There are, however, no large changes in ellipticity between adjacent isophotes and there is no evidence for isophotal twisting, suggesting that the host is undisturbed. There is insufficient IR photometry to draw any conclusions concerning the IR power source.

4.5.5 *F12358+1807*

$z = 0.45$. This moderately bright QSO shows no signs of tidal interaction, the surrounding nebulosity being extremely symmetric. There is, however, a bright spiral galaxy 8.6 arcsec to the north, the magnitude of which ($m_{814} = 20.05$) suggests that it may be a companion rather than a chance foreground object. The spiral appears to be morphologically undisturbed and the spatial separation between it and the source is too great for direct interactions. The IR power source of this object cannot be constrained as there is insufficient IR photometry available.

The host galaxy is formally detected at >99 per cent confidence and an elliptical profile is strongly preferred to a spiral profile ($\chi^2 \sim 1.0$ versus $\chi^2 \sim 4.0$). Fitting elliptical isophotes shows that the ellipticity is of the order of 0.1–0.2. The host has an absolute k-corrected magnitude of -24.5 and a derived scalelength of 7.1 kpc.

4.5.6 *F12509+3122*

$z = 0.78$. This QSO is very symmetrical and shows no signs of interaction. There is, however, a large, bright companion galaxy 15.5 arcsec to the south, the magnitude of which ($m_I = 17.9$) suggests physical association with the source rather than chance spatial coincidence. The companion appears to be morphologically undisturbed, but has a bright nucleus. The light distribution of the companion is best fitted by an elliptical profile, the *HST* image suggests it may be an S0 galaxy. Interestingly, this galaxy, if it is a companion, has a comparable magnitude ($M_I = -25.2$) to the QSO host galaxies, and is also similar to the brightest ellipticals found in moderate to rich galaxy clusters. In addition to the bright companion there are also four other smaller, dimmer companion sources.

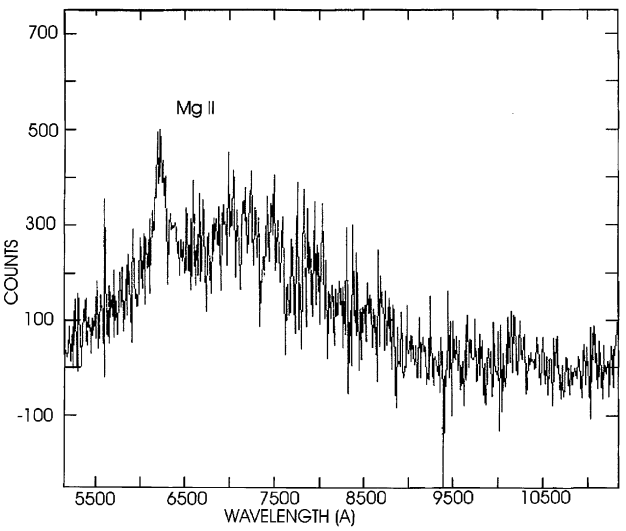

Figure 5. Optical spectrum for F14218+3845, taken by Andy Lawrence with the FOS-I spectrograph on the Isaac Newton Telescope as part of the *IRAS* FSS-z survey.

© Royal Astronomical Society • Provided by the NASA Astrophysics Data System

2002MNRAS.329..605F

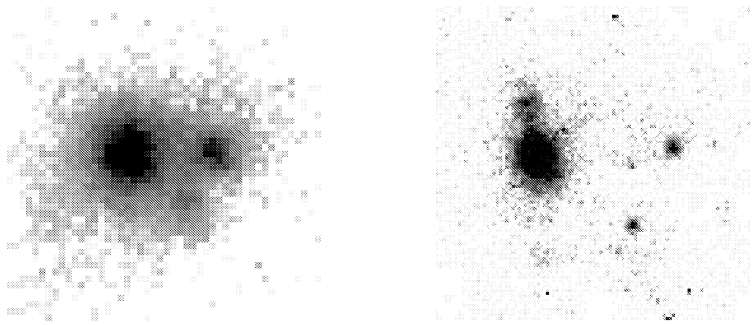

Figure 6. *Keck K*-band image of F15307+3252 (left-hand panel, supplied by Liu) and *HST I*-band image. Orientation and scale are the same as in Fig. 2.

The host galaxy is formally detected with >97.5 per cent confidence, has an absolute k-corrected magnitude of −25.2, and a scalelength of 10.3 kpc. The 60−25 μm colour suggests that an AGN interpretation of the IR SED is most likely, although previous studies (Rowan-Robinson 2000) imply an unquantified, but significant starburst component. The measured ellipticity of the host was found to be small, $\langle\epsilon\rangle = 0.15$.

4.5.7 *F14218+3845*

$z = 1.21$. Overall, the IR emission from this object is best explained as being predominantly (74 per cent) starburst in origin (Verma et al. 2001). The starburst dominates only at wavelengths longward of 30 μm. Below 30 μm the AGN torus dominates. The fit predicts that an AGN should be responsible for most of the optical emission, which is consistent with the optical morphology. The optical spectrum of this source, taken as part of the *IRAS* FSS-z survey (Oliver et al. 1996) on the Isaac Newton Telescope using the Faint Object Spectrograph (FOS-I), is given in Fig. 5. The single broad line is most plausibly interpreted as Mg II. Another possibility is Hβ, but the absence of an Hα line at longer wavelengths makes this interpretation unlikely. There are two small dim companions 5.8 arcsec away to the south-east and south-west, and one slightly more extended companion 13.5 arcsec to the south-west. The source itself is very small. A host galaxy was detected at >99 per cent confidence, although it proved impossible to distinguish between a de Vaucoleurs or spiral galaxy profile as both profiles produced an equally good fit to the data. The host galaxy magnitude ($M_I = -24.7$) is much closer in value to the total source magnitude than for any of the other sources. There is an extremely faint inhomogeneity ∼0.5 arcsec to the south-east in the form of a very small plume of nebulosity, this feature is, however, barely detected in the *HST* image (∼3σ) and the PSF subtracted image shows no signs of disturbance. We thus conclude that this object is not involved in ongoing interactions.

On *prima facie* grounds, the *HST* image of this source shows possible gravitational lensing signatures. Further investigation, however, showed no evidence for lensing. The very faint 'ring' surrounding the QSO is at the same radius as the Airy ring in the normalized TINYTIM PSF generated for this object, and is therefore virtually certain to be a PSF-artefact. The likelihood of seeing a symmetrical Einstein ring with perfectly uniform luminosity around the entire circumference is in any case fairly small, and would require perfect or near-perfect alignment between a circularly symmetric lens and an extended source. There is no tangential stretching of the source, and there are no other structures or nearby companions that suggest any plausible lensing scenario. This implies that the derived IR luminosity is intrinsic to the source.

4.5.8 *F15307+3252*

$z = 0.93$. This object was first identified as an HLIRG by Cutri et al. (1994). It was, after F10214+4724 and P09104+4109, the third HLIRG to be discovered, and bears many similarities to its predecessors. Optical spectropolarimetry by Hines et al. (1995) shows a highly polarized continuum, and a broad emission-line region that is typical of QSOs. Nearby companions have been detected in K-band images (Soifer et al. 1994). Liu, Graham & Wright (1996) discuss the properties of this object and, using deep *Keck K*-band imaging combined with 1.1−1.4 μm spectroscopy, discuss whether this object is gravitationally lensed or a giant elliptical in the process of formation. Their results are inconclusive. *ROSAT* High Resolution Imager (HRI) observations (Fabian et al. 1996) show no X-ray emission down to a limit of $2\times10^{-4}L_{\rm bol}$, indicating either atypically weak X-ray emission or that little of the X-ray flux is scattered into our line of sight.

CO line and rest frame 650-μm observations (Yun & Scoville 1998) derive upper limits to the CO molecular gas mass of $5\times10^9\,{\rm M}_\odot$, and a dust mass of $0.4-1.5\times10^8\,{\rm M}_\odot$. Both of these values are lower than those typical for the more gas-rich IR galaxies. Further observations of this object show a Seyfert 2 spectrum (Cutri et al. 1994). This was later confirmed by mid-IR spectroscopy (Evans et al. 1998), which also found a molecular gas mass comparable to or less than that found in the most gas-rich galaxies observed locally, that the relatively 'warm' 60/100 μm colours imply that most of the IR emission emanates from a relatively small amount of warm circumnuclear dust ($M_{\rm dust} = 10^5-10^7\,h^{-2}\,{\rm M}_\odot$, which implies a molecular gas mass $M_{\rm gas} =$

Table 3. Photometry for features within F15307+3252.

No	Flux (mJy)	m_I	M_I[a]	m_K[b]
1	5.7×10^{-3}	18.7	−24.8	17.6
2	1.1×10^{-3}	21.9	−21.6	18.2
3	2.6×10^{-4}	22.2	−21.3	20.1

1 refers to the large north-western source,
2 refers to the small south-eastern source and
3 refers to the small north-eastern source.
The two companion sources clearly possess different $I-K$ colours, ruling out a quadruple lensing scenario.
[a]No applied k-correction.
[b]Taken from Liu et al. (1996).

© Royal Astronomical Society • Provided by the NASA Astrophysics Data System

2002MNRAS.329..605F

$10^{7.3}-10^{9.3}\,h^{-2}\,M_{\odot}$), and that the narrow emission lines and $L_{ir}/L_{bol}=0.90$ imply that the AGN is mostly obscured. The non-detection of CO poses a problem for a purely starburst interpretation (Rowan-Robinson 2000), and IR SED modelling (Verma et al. 2001) implies that an AGN is responsible for the majority (68 per cent) of the IR emission.

The *HST* image shows an interacting system with three bright components. The most prominent source is large, bright, and has some small, bright arclike structures immediately to the south-west. The two smaller components are located 1.9 arcsec to the south-east, with the southerly one being noticeably brighter than the northern one. Extremely faint, diffuse emission is also present surrounding all three components. There is one small dim companion and one small bright companion 7.3 and 13.2 arcsec to the south, respectively.

The extremely high-resolution image of this source taken by *HST*, in conjunction with the *Keck K*-band image, allows the best possible chance for determining whether or not this system is lensed. Both the *Keck* image (see also fig. 3 of Liu et al. 1996) and the *HST I*-band image are given for comparison in Fig. 6. The two possible lensing scenarios given by Liu et al. are:

(i) the large, bright elliptical component is the lensed nuclear structure of a $z=0.93$ galaxy, with the brighter of the two companion sources being the foreground lens;

(ii) this source is a quadruple image gravitational lens system; by comparing the *HST* image with the *Keck* image (kindly provided by Liu) it is possible to examine both of these possibilities.

We first examine the possibility of a quadruple image gravitational lens system. First, there is no evidence from the *I*-band image for the lens itself, although this in particular does not help to rule out a lensing scenario. Table 3 gives the magnitudes in the *I* and *K* bands for the three components in the system observed in both the *HST* and *Keck* images. The two smaller sources in the system possess different $I-K$ colours. Although differential reddening through a foreground lens could account for colour differences between the four components the 'arclike' structures to the south-west of the large elliptical component would be expected to be reddened in comparison with the other three components in the system if this were the case. Instead they are observed to be significantly bluer as they do not appear at all in the *K*-band image, but are prominent in the *I*-band image. The large, bright elliptical component does not appear stretched tangentially, but shows both radial and tangential extension. Explaining radial extension in a quadruple image gravitational lens is not possible unless extremely complex lensing scenarios are invoked, scenarios that are not plausible from the evidence in the *I*-band image. Although a quadruple lens scenario cannot be completely ruled out, it seems overwhelmingly unlikely.

If the bright elliptical component of the system is assumed to be the lensed galaxy, with the brighter of the two companion sources assumed to be the lens, then the lack of counter images to the south of the lens is difficult to explain. The smaller of the two companion sources cannot be such a counter image as it appears on the same side of the lens as the bright elliptical, such a scenario would require unrealistic amounts of cosmic shear. This rules out the possibility that the large, bright elliptical component is the lensed nuclear structure of a $z=0.93$ galaxy, with the brighter of the two companion sources being the foreground lens. We conclude therefore that this object is not gravitationally lensed and that the IR emission is intrinsic to the source.

Fitting elliptical isophotes to the largest component in this source shows that the ellipticity varies over $0.25<\epsilon<0.4$ as the radius varies over $0.2<r<0.32$ in arcsec. The best-fitting profile of the large bright component is found to be an elliptical, with an associated scalelength of 12.4 kpc and an absolute *k*-corrected magnitude of $M_I=-26.4$.

4.5.9 *PG1634+706*

$z=1.33$. This radio-quiet object is the most IR luminous optically selected QSO in the *IRAS* catalogues. The extraordinarily high disc luminosity ($\sim 10^{40}\,W\,s^{-1}$) requires a central black hole of $10^{10}\,M_{\odot}$, even at the Eddington accretion limit (Rachen, Mannheim & Biermann 1996). An AGN dust torus model is consistent with both the *ISO* (Haas et al. 1998) and *IRAS* data, with a limit set on any starburst contribution, a limit that is confirmed by the non-detection of CO (Evans et al. 1998). The near IR spectrum (Evans et al. 1998) is not consistent with a Seyfert 2 galaxy, and the derived molecular gas mass is comparable to or less than that found in the most gas-rich galaxies observed locally. They also find that the relatively 'warm' 60/100 μm colours imply that most of the IR emission emanates from a relatively small amount of warm circumnuclear dust ($M_{dust}=10^{5}-10^{7}\,h^{-2}\,M_{\odot}$, implying a molecular gas mass $M_{gas}=10^{7.3}-10^{9.3}\,h^{-2}\,M_{\odot}$), and that the broad emission lines and $L_{ir}/L_{bol}=0.35$ suggests that most of the AGN is exposed. *ASCA* spectroscopy of this object (Nandra et al. 1995) agrees with these conclusions to some extent. Both the Fe Kα line and 'hard tail' are not present in the spectrum, features that are almost universal in Seyfert 2 galaxies. The accretion disc is thus concluded to be either highly ionized or optically thin, both of which would indicate that accretion is occurring close to or at the Eddington accretion limit. An optically thick molecular torus is concluded to be either absent or subtending a small angle to the X-ray source. *ROSAT* PSPC observations (Rachen et al. 1996) show this source to have a steep soft X-ray slope, a natural explanation of which is that the soft X-ray emission is of unsaturated comptonization origin, covered by a flat non-thermal X-ray component above 1.4 ± 1.1 KeV. Barvainis, Lonsdale & Antonucci (1996) confirm previous radio observations of this source that show a high-frequency excess, attributed to a compact synchrotron source most commonly found in radio-loud objects.

The *HST* image shows a large, bright, symmetrical source with no surrounding nebulosity. There are no companions within the 36-arcsec field of view. A host galaxy was detected for this object, and a spiral disc profile is preferred over an elliptical profile. The host was, however, only detected at ~80 per cent confidence over a pure PSF fit, and the derived host galaxy magnitude, at $M_I=-29.4$, is also unphysical. It is therefore more likely, as in the case of PG1148+549 that we are merely detecting a profile of scattered light from the AGN and that the host galaxy is unresolved. The IR SED is dominated by the AGN torus component (83 per cent), with line-of-sight inclination of 90°. The starburst model of age 6.6 Myr and $\tau_{UV}=220$ is required only to explain the emission longward of 60 μm.

5 DISCUSSION

5.1 The sources

5.1.1 *Morphology*

On an ad hoc basis the sample can be divided into two groups on the basis of their morphology, namely an 'interacting' group and a

© Royal Astronomical Society • Provided by the NASA Astrophysics Data System

2002MNRAS.329..605F

'quasar' group. The 'interacting' group comprises three objects; F00235+1024 and F15307+3252 are both strongly interacting, F10026+4949 shows slightly weaker signs of interaction but has numerous nearby (<5 arcsec) companions. The 'quasar' group comprises the other six sources, five of which are optically bright QSOs and one of which, F14218+3845, is a QSO where the point source is relatively underluminous.

There is a strong morphological resemblance between the 'interacting' group of HLIRGs and previous *HST* imaging of ULIRGs (Surace et al. 1998; Borne et al. 2000). The strong resemblance between three sources in this sample with previously observed interacting ULIRGs, and that the rest of the sources are QSOs, raises the question as to whether any of the QSOs in the sample have arisen from interactions or mergers. It has been suggested (Sanders et al. 1988) that ULIRGs represent a transition phase between galaxy mergers and optically luminous quasars. The formation of quasar nuclei in ULIRGs has been investigated by Taniguchi, Ikeuchi & Shioya (1999). They conclude that a supermassive black hole (SMBH) of mass $\geq 10^8\,M_\odot$ can form if either one of the progenitor galaxies contains a 'seed' SMBH of mass $\geq 10^7\,M_\odot$ undergoing efficient Bondi-type gas accretion during the merger, or by collapse of some star cluster containing compact remnants (black holes or neutron stars) on a time-scale of $\sim 10^9$ yr. A more recent study of ULIRGs (Farrah et al. 2001) using *HST*, proposes that ULIRGs as a class are not simply a transition stage between galaxy mergers and QSOs, but instead are a much more diverse population the evolution of which is driven solely by the morphologies of the merger progenitors and the local environment.

Signs of interaction in the immediate vicinity of the QSOs in the sample would be hard to detect owing to the bright central source, and the relatively high redshifts of the objects. A significant fraction of ULIRGs in which QSO activity is apparent have shown clear signs of interactions (Leech et al. 1994; Clements et al. 1996), and observations of QSOs from the PG quasar survey (Clements 2000) showed that QSOs with disturbed hosts were significantly more likely to have a higher FIR luminosity than those QSOs with undisturbed hosts. These studies have, however, involved objects at redshifts ≤ 0.2. Of the six QSOs in this sample, three show faint signs of morphological disturbance, two are apparently undisturbed and one (PG1634 + 706) is too distant to tell. Given that all the objects that do not have an optical QSO show clear signs of interaction, and that the other six are QSOs it seems plausible that the QSOs in the sample could represent the final stage in a merger event. HLIRGs would then be plausibly interpreted as a simple extrapolation of the ULIRG population to extreme luminosities. From the *HST* and IR data alone it is, however, not possible to rule out that some or all of the QSOs are not a simple extrapolation of the ULIRG population to extreme luminosities and that the IR emission is not triggered by interactions.

5.1.2 *An optical/IR comparison*

The IR power sources for those objects with previously modelled 1–1000 μm IR SEDs can be found in Table 1. For the five sources with sufficiently comprehensive IR photometry to allow detailed modelling of the IR SED, two are starburst-dominated and three are AGN-dominated, although all five require both a starburst and an AGN to explain the IR emission. Two sources with less comprehensive IR photometry that cannot be modelled using detailed SED models show evidence for an AGN dominating the IR emission, with a smaller, but unquantified contribution from a starburst. The remaining two sources have an unknown IR power source as they have only one IR data point.

Table 1 gives a direct comparison between the *HST* morphology and the best-fitting model with the IR SED. Of the two sources that are starburst-dominated, one (F00235+1024) is interacting and the other (F14218+3845) is a QSO. For the five systems where an AGN is the dominant IR power source, two (F10026+4949 and F15307+3252) are strongly interacting and the rest are QSOs. It can be argued that all the starburst systems are triggered by interactions, one is in ongoing interactions, whilst the second (F14218+3845) shows no clear signs of interaction but does possess close companions. For the five AGN-dominated systems, however, two are in ongoing interactions, but three are optically luminous QSOs with no signs of interaction or very close companions. There is therefore no clear correlation between the IR power source and the optical morphology in this sample of HLIRGs. The number of sources considered here is, however, too small to draw truly robust statistical constraints on the HLIRG population. This means that these conclusions are by nature quite speculative, and should be regarded with some caution.

For the five sources with well-sampled SEDs, the optical morphology correlates well with that predicted by the dominant contributor to the SED in the optical. For PG1148+549, F14218+3845 (Verma et al. 2001) and PG1634+706, the SED fit predicts that the optical emission is dominated by an AGN, which is in excellent agreement with the optical images. For F00235+1024 and F15307+3252 (Verma et al. 2001) the SED fit predicts that the AGN do not contribute significantly to the optical emission. Although the unquantified contribution from old stellar populations to the *I*-band flux means that the optical data cannot be used to constrain the properties of the starburst, the absence of AGN both in the optical images and in the optical region of the SED are consistent with each other.

A colour–colour plot [$\log(S_{25}/S_{60})$ versus $\log(S_{60}/S_{814})$] for the nine sources in the sample can be found in Fig. 7. All of the optically luminous QSOs are localized in the bottom right-hand corner of the colour–colour plane. The three interacting sources are also localized in the $\log(S_{60}/S_{814})$ axis, but are more spread out along the $\log(S_{25}/S_{60})$ axis owing to their varied AGN fractions.

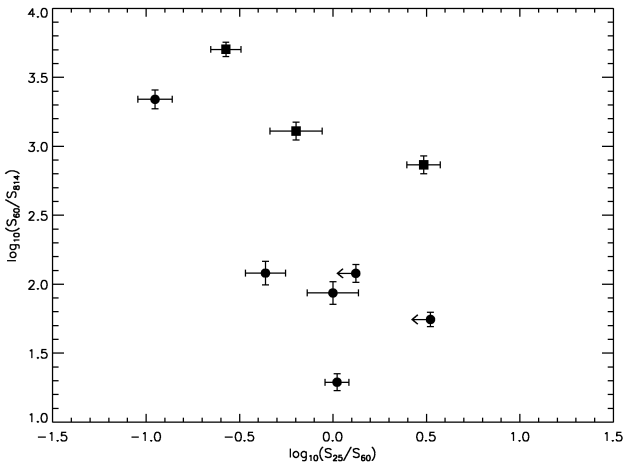

Figure 7. Colour–colour plot for the nine sources in the sample. *K*-corrections have been applied to the *I* band and IR fluxes so that the plot approximates rest-frame colours. The circles are those sources classified as QSOs on the basis of their optical spectra, and the squares are the interacting sources.

© Royal Astronomical Society • Provided by the NASA Astrophysics Data System

2002MNRAS.329..605F

F14218+3845 is both substantially less luminous in the optical compared with the other QSOs in the sample (probably owing to higher levels of obscuration in the nuclear regions), and contains a starburst component contributing dominantly to the IR emission longward of 60 μm (Verma et al. 2001), hence its position in the top left-hand side of the colour–colour plane close to the interacting sources.

5.1.3 *Gravitational lensing*

The extraordinarily high bolometric IR luminosities observed in these objects suggests that magnification via gravitational lensing may play a significant role. Gravitational lensing has been observed previously in four IR selected hyperluminous sources, these include the 'Cloverleaf' quasar and F10214+4724. Signs of lensing were therefore a primary search objective for this sample. One of the sources was known to be a strong candidate for lensing, as morphological information for F15307+3252 from ground-based imaging suggested that it may be a lensed system of some kind (Liu et al. 1996).

It came as quite a surprise therefore, when none of the sources in the sample showed any evidence for gravitational lensing. The previous observations of HLIRGs that have detected lensing using *HST* indicate that this phenomenon is at least present to some extent in the HLIRG population. Including our sample suggests that only a small minority (around 15–20 per cent) of HLIRGs have been mistakenly classified as such owing to the effects of lensing. This percentage should be treated with a degree of caution; the sample presented here is at a lower median redshift than that of previously confirmed lensed sources, the sample of *HST*-imaged HLIRGs is also as a whole not homogenous. There is also the possibility that these objects may be lensed by a foreground cluster, such a lensing scenario might be expected to produce weaker signs of lensing than would be observed if any of these objects were being lensed by a single source. This possibility can only be fully examined by a quantitative study of the environments of these objects, although the complete lack of lensing signatures in any of the objects makes a cluster lens scenario unlikely.

5.2 The host galaxies

Previous surveys of QSOs using *HST* have generally been extremely successful in detecting host galaxies. Urry et al. (1999), give results for a sample of BL Lacertae objects, detecting host galaxies out to a redshift of $z = 0.7$. They find that the hosts are all extremely luminous ellipticals with $\langle M_I \rangle = -24.6$. The derived ellipticities are generally low and morphologies are smooth. Imaging of a sample of 14 quasars (six radio-loud, five radio-quiet, three radio-quiet ultraluminous infrared quasars) by Boyce et al. (1998) showed that all the radio-loud quasars had elliptical hosts, the radio-quiet quasars possessed both elliptical and spiral hosts, and that the radio-quiet ultraluminous infrared quasars lay in violently interacting systems. Host galaxies were on average 0.8-mag brighter than L^*. *K*-band imaging of a sample of 14 luminous radio-quiet QSOs (Percival et al. 2001) found that two of the host galaxies were violently interacting, and the rest were undisturbed ellipticals. Results from imaging of two luminous radio-quiet quasars (Bahcall, Kirhakos & Schneider 1996) show that both quasars reside in apparently normal host galaxies, one being an elliptical and one a spiral. Disney et al. (1995) present *HST* imaging for a sample of four QSOs, finding that all four have elliptical hosts. Although they find that the morphologies of the hosts are all featureless they argue that the presence of multiple very close companions is evidence for interactions as the trigger for the quasar activity.

We resolved host galaxies in seven of the nine objects, with the host morphology being resolved in five of those cases. Host properties were reliably determined up to a redshift of 0.78, except in the case of F14218+3845, where the relatively underluminous point source allowed determination of the host galaxy magnitude, but not the profile. The host galaxy was not resolved for the two PG quasars, probably because the extremely bright central source in these two objects creates a profile of scattered light that completely masks the host galaxy. The morphology of F00235+1024 was also too disturbed to fit a galaxy profile.

The five reliably resolved profiles were all best fitted by an elliptical profile with at least 97.5 per cent confidence. The average QSO host galaxy magnitude was found to be $\langle M_I \rangle = -24.9$, more than 1.7-mag brighter than L^*. For those sources that do not display a point source the galaxies were brighter, with $\langle M_I \rangle = -25.5 \pm 0.9$. The derived scalelengths were also large, all but one falling in the range $6.7 < r_e < 12.5$. The scalelength for LBQS1220+0939, at ~88 kpc is extremely large, and is comparable to the largest observed ellipticals. The possibility exists that this value is erroneous, possibly owing to AGN light scattered within the host galaxy or (less likely) a poorly subtracted PSF, however, the faint, extended emission surrounding this source is supportive of a large scalelength.

We simulations performed to quantify the efficiency of host galaxy detection, and to determine whether signs of morphological disturbance would be resolved after PSF subtraction. In order to make the simulations realistic we took the large bright elliptical component of F15307+3252, which shows weak signs of morphological disturbance, and added on an observed saturated PSF taken with the F814W filter from the *HST* PSF archive. TINYTIM PSFs were then generated for the position of this observed PSF. Subtraction and fitting procedures were carried out as for the QSOs in the sample. A host galaxy was detected at >97.5 per cent

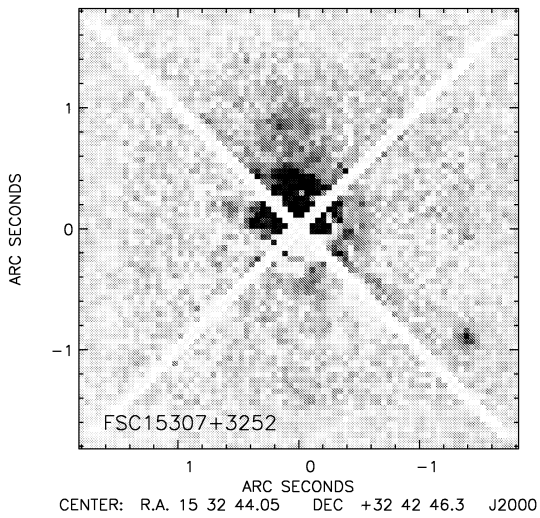

Figure 8. A simulation in which an observed, saturated Planetary Camera *I*-band PSF is added to the large elliptical component of F15307+3252 shown in Fig. 2. A theoretical TINYTIM PSF has then been subtracted off, following the procedures described in Section 3.2. Residual PSF features have been masked out. The weak signs of morphological disturbance seen in the original image are still clearly visible. The less luminous of the two companion sources is visible on the lower right-hand side of the image.

© Royal Astronomical Society • Provided by the NASA Astrophysics Data System

2002MNRAS.329..605F

confidence, and an elliptical profile was clearly preferred to a spiral profile. The measured host galaxy magnitude was found to be $M_I = -24.9 \pm 0.2$, with an associated scalelength of $r_e = 12.8 \pm 0.8$ kpc. The 1σ errors of both of these values lie within the original derived values for this object. Fig. 8 shows the galaxy after PSF subtraction. The signs of disturbance in the original image are still clearly visible. We therefore conclude that, had any of the detected host galaxies of the QSOs shown signs of interaction of a level comparable to that seen in the large elliptical component of F15307+3252, we would have detected them.

The derived host galaxy properties are similar to the properties of the hosts of BL Lac objects observed by Urry et al. They are also similar to the host galaxy properties derived for radio-quiet QSOs by Boyce et al. and Bahcall et al., although we do not find any spiral hosts. Observations of the brightest ellipticals in the Virgo and Coma clusters (Caon et al. 1994; Jorgensen & Franx 1994) show that they have very similar properties to our host galaxies. Interestingly, both *IRAS* quasars imaged by Boyce et al. had host galaxies classified as interacting. If all the QSOs in our sample arose owing to interactions and mergers it would not be unreasonable to expect some of the hosts in our sample to be interacting systems, although the combination of a luminous point source and relatively high redshift may well serve to mask any such features. The low measured ellipticities for the QSO hosts suggests that the hosts are either featureless or in the very last stages of a merger. As ULIRGs are thought to be mergers between two or more gas-rich spiral galaxies, and as a merger between two such galaxies is thought to form an elliptical galaxy (Barnes 1989), the properties of our host galaxies are consistent with being ULIRGs in the final stages of a merger.

5.3 Companion sources

It has long been suspected that IR emission in ULIRGs is triggered by interactions and mergers (Sanders & Mirabel 1996), one possibility (Borne et al. 2000) is that the IR emission may arise because of multiple mergers and interactions in Hickson compact groups. Results from the analysis of the QSO host galaxies suggest that HLIRGs may reside in rich clusters, given that the hosts are very similar to the brightest cluster ellipticals observed locally. All but one of the samples show at least one companion source within 36 arcsec. Two sources have single, large, nearby bright companions, one of which is a very bright elliptical, the other being a spiral. The other six all show at least two smaller, dimmer companions within a 16-arcsec radius. The one exception, PG1634+706, apparently has no companions within 0.5 Mpc, suggesting that this source does not reside in a cluster.

These results, even when taken in conjunction with the results for the host galaxies, do not provide conclusive evidence for or against a cluster environment for all HLIRGs, but do suggest that some HLIRGs may reside in a rich environment. The environments of the HLIRGs in this sample will be presented in more detail in a future paper.

Studies of the environments of ULIRGs (Borne & Scott 1991; Sanders 1992) have shown that these objects do not appear to reside in regions of higher than average density. Most ULIRGs appear either isolated or in systems that are similar to the local group. Results from the *IRAS* surveys have shown that most ULIRGs are strong interactions between gas-rich spirals with a relative mean velocity of $\leq 200\,\mathrm{km\,s^{-1}}$. These are not typical conditions of rich cluster environments, where relative mean velocities are much higher and many galaxies are either gas-poor spirals, or ellipticals (Sanders & Mirabel 1996). A study of the cluster environments of radio-loud and radio-quiet AGN has been performed by Mclure & Dunlop (2001). They showed that both classes of object resided in rich environments of approximately Abell class 0, although there was a large scatter. They also found no evidence for an epoch dependent change in the environments, and that AGN cluster environments as a whole were consistent with being drawn at random from the general cluster population.

The tentative hypothesis presented here that some fraction of HLIRGs may reside in a rich cluster environment, if confirmed, would be an important result and would raise problems for interpreting HLIRGs as a simple extrapolation of the *IRAS* galaxy population to extreme luminosities. Density evolution with redshift cannot explain sparse environments at $z \sim 0.2$ and rich environments at higher redshift. In any case strong luminosity evolution, as opposed to density evolution, is most appropriate for explaining faint radio source counts (Rowan-Robinson et al. 1993). HLIRGs may be the cluster analogues of ULIRGs; the higher relative mean velocities found in rich clusters would make the merger-driven IR luminous phase shorter, this would also provide a formation mechanism for cluster elliptical galaxies. This scenario would imply some correlation between luminosity and environment in the more luminous of the *IRAS* galaxies. Alternatively, HLIRGs may be an entirely separate class of object.

6 CONCLUSIONS

We have performed *HSTI*-band imaging for a sample of nine hyperluminous infrared galaxies. The results given as follows.

(i) The morphologies in the sample include both strongly interacting systems and QSOs with no clear signs of ongoing interaction.

(ii) No source in the sample shows any evidence for gravitational lensing. This includes F15307+3252, for which lensing had been previously suspected. Lensing is thus concluded to be entirely absent from the sample or at such a low level that it has a negligible impact on the observed luminosities.

(iii) The QSO host galaxies are all extremely luminous ellipticals with properties comparable to the brightest cluster elliptical galaxies observed locally.

(iv) There is no clear correlation between the IR power source and the optical morphologies. Of the seven sources with enough IR photometry to investigate the IR power source, two are starburst-dominated and five are AGN-dominated, although all seven show evidence for some level of AGN emission. One of the starburst-dominated systems is in ongoing interactions, the other is a QSO with close companions. Of the five AGN-dominated systems, two are interacting and three are QSOs with no signs of interaction. There is, however, good agreement between the optical morphologies and the dominant contributor to the optical emission predicted by the SED.

(v) Two of the sources in the sample show a single bright companion, six show at least two small dim companions. One source is very probably isolated.

Previous observations of HLIRGs have seen evidence for amplification of intrinsic luminosities via gravitational lensing. None of our sources, however, showed any evidence for this phenomenon, including one for which lensing had been previously strongly suspected. We conclude that only a small minority (perhaps 15–20 per cent) of HLIRGs have been misclassified owing to gravitational lensing.

© Royal Astronomical Society • Provided by the NASA Astrophysics Data System

2002MNRAS.329..605F

These results are consistent with the majority of the HLIRG population constituting the extremely bright end of the ULIRG population, i.e. where interaction-induced star formation and quasar activity lead to the very high IR luminosities. The evidence for this can be summarized as:

(i) three of the sources lie in interacting systems, which bear a strong morphological resemblance to ULIRGs;

(ii) for the five sources with sufficient data to accurately model the IR SED, the IR emission is best explained as arising from a mixture of starburst and AGN activity, which is similar to that found amongst ULIRGs;

(iii) the QSO host galaxy properties correspond closely to locally observed bright cluster ellipticals, a cluster environment would provide a convenient source for interactions and mergers;

(iv) most of the sources show at least two nearby companions;

(v) one of the bright companion sources is a galaxy with similar properties to bright cluster ellipticals.

There are, however, some important points to note concerning these conclusions. None of the QSOs or QSO hosts show any clear signs of interaction, signs that have been observed in ULIRGs in which QSO activity is apparent. Such signs may, however, be hidden because of high redshift, luminous central source, or because hyperluminous activity takes place in mid-to-late stage mergers where the signs of merging are diminished. The evidence that the QSOs reside in luminous elliptical hosts is only suggestive that some may also reside in rich cluster environments, and is not conclusive. For example, one source (PG1634+706) is apparently isolated. Further analysis is required to make more concrete statements concerning the local environments of HLIRGs. If the tentative suggestion put forward here that some HLIRGs may reside in a rich cluster environment is found to be correct, then this would pose problems for HLIRGs being a simple extrapolation of ULIRGs to extreme luminosities as ULIRGs are known not to reside in rich clusters. It is thus possible that some HLIRGs are the cluster analogues of ULIRGs, or that the IR emission in some HLIRGs may not be triggered by interactions.

It must be emphasized that these conclusions are based on a relatively small sample of objects, essentially those HLIRGs that have been observed at sufficient resolution to reliably determine morphologies, host galaxy properties and lensing characteristics. It is not possible to draw statistically significant conclusions from a sample of this size. Observations of a larger number of HLIRGs to the highest possible depth and resolution are the only way to confirm or refute the conclusions drawn above.

ACKNOWLEDGMENTS

We would like to thank Stephen Serjeant and John Krist for invaluable advice on PSF subtraction, Stephen Warren for advice both on PSF subtraction and gravitational lensing, John Biretta and Stefano Casertano for assistance with data reduction and analysis, Andreas Efstathiou for helpful discussions and for providing the IR SED models, and Michael Liu for providing the *Keck* image of F15307+3252. The data presented here were obtained using the NASA/ESA *Hubble Space Telescope*, obtained at the Space Telescope Science Institute, which is operated by the Association of Universities for Research in Astronomy, Inc., under NASA contract NAS 5-2655. The work presented has made use of the NASA/IPAC Extragalactic Data base (NED), which is operated by the Jet Propulsion Laboratory under contract with NASA. The Isaac Newton Telescope is operated on the island of La Palma by the Isaac Newton Group in the Spanish Observatorio del Roque de los Muchachos of the Instituto de Astrofisica de Canarias. DGF would like to acknowledge the award of tuition fees and maintenance grant provided by the Particle Physics and Astronomy Research Council. This work was in part supported by PPARC grant no GR/K98728.

REFERENCES

Bahcall J. N., Kirhakos S., Schneider D. P., 1996, ApJ, 457, 557
Barbieri C., Cappellaro E., Turatto M., Romano G., Szuszkiewicz E., 1988, A&AS, 76, 477
Barnes J., 1989, Nat, 338, 132
Barvainis R., Lonsdale C., Antonucci R., 1996, A&AS, 188, 2305
Borne K. D., Scott J. H., 1991, STScI Conf. Ser., Vol 5, Massive Stars and Starbursts. Cambridge Univ. Press, Cambridge
Borne K. D., Bushouse H., Lucas R. A., Colina L., 2000, ApJ, 529L, 77
Boyce P. J. et al., 1998, MNRAS, 298, 121
Broadhurst T., Lehar J., 1995, ApJ, 450L, 41
Brown R. L., vanden Bout P. A., 1991, AJ, 102, 1956
Caon N., Capaccioli M., D'Onofrio M., 1994, A&AS, 106, 199
Clements D. L., 2000, MNRAS, 311, 833
Clements D. L., Sutherland W. J., McMahon R. G., Saunders W., 1996, MNRAS, 279, 477
Cutri R. M., Huchra J. P., Low F. J., Brown R. L., vanden Bout P. A., 1994, ApJ, 424L, 65
de Grijp M. H. K., Miley G. K., Lub J., de Jong T., 1985, Nat, 314, 240
Disney M. J. et al., 1995, Nat, 376, 150
Efstathiou A., Rowan-Robinson M., 1995, MNRAS, 273, 649
Efstathiou A., Hough J. H., Young S., 1995, MNRAS, 277, 1134
Efstathiou A., Rowan-Robinson M., Siebenmorgen R., 2000, MNRAS, 313, 734
Efstathiou G., Ellis R. S., Peterson B. A., 1988, MNRAS, 232, 431
Eisenhardt P. R., Armus L., Hogg D. W., Soifer B. T., Neugebauer G., Werner M. W., 1996, ApJ, 461, 72
Elston R., McCarthy P. J., Eisenhardt P., Dickinson M., Spinrad H., Januzzi B. T., Maloney P., 1994, AJ, 107, 910
Evans A. S., Sanders D. B., Cutri R. M., Radford S. J. E., Surace J. A., Solomon P. M., Downes D., Kramer C., 1998, ApJ, 506, 205
Fabian A. C., Cutri R. M., Smith H. E., Crawford C. S., Brandt W. N., 1996, MNRAS, 283L, 95
Farrah D. et al., 2001, MNRAS, 326, 1333
Fioc M., Rocca-Volmerange B., 1997, A&A, 326, 950
Graham J. R., Liu M. C., 1995, ApJ, 449L, 29
Green S. M., Rowan-Robinson M., 1996, MNRAS, 279, 884
Griffiths R. E. et al., 1994, ApJ, 437, 67
Haas M., Chini R., Meisenheimer K., Stickel M., Lemke D., Klaas U., Kreysa E., 1998, ApJ, 503L, 109
Hamann F., Shields J. C., Ferland G. J., Korista K. T., 1995, ApJ, 454, 688
Hines D. C., Schmidt G. D., Smith P. S., Cutri R. M., Low F. J., 1995, ApJ, 450L, 1
Holtzman J. A., Burrows C. J., Casertano S., Hester J. J., Trauger J. T., Watson A. M., Worthey G., 1995, PASP, 107, 1065
Jorgensen I., Franx M., 1994, ApJ, 433, 553
Kleinmann S. G., Hamilton D., Keel W. C., Wynn-Williams C. G., Eales S. A., Becklin E. E., Kuntz K. D., 1988, ApJ, 328, 161
Krist J., 1995, ADASS, 4, 349
Lawrence A. et al., 1993, MNRAS, 260, 28
Leech K. J., Rowan-Robinson M., Lawrence A., Hughes J. D., 1994, MNRAS, 267, 253
Liu M. C., Graham J. R., Wright G. S., 1996, ApJ, 470, 771
McLure R. J., Dunlop J. S., 2001, MNRAS, 321, 515
Nandra K., Fabian A. C., Brandt W. N., Kunieda H., Matsuoka M., Mihara T., Ogasaka Y., Terashima Y., 1995, MNRAS, 276, 1
Oliver S. J. et al., 1996, MNRAS, 280, 673

© Royal Astronomical Society • Provided by the NASA Astrophysics Data System

2002MNRAS.329..605F

Percival W. J., Miller L., McLure R. J., Dunlop J. S., 2001, MNRAS, 322, 843
Poggianti B. M., 1997, A&AS, 122, 399
Pozzetti L., Bruzual A. G., Zamorani G., 1996, MNRAS, 281, 953
Rachen J. P., Mannheim K., Biermann P. L., 1996, A&A, 310, 371
Rana N. C., Basu S., 1992, A&A, 265, 499
Ratnatunga K. U., Griffiths R. E., Ostrander E. J., 1999, AJ, 117, 2010
Rowan-Robinson M., 2000, MNRAS, 316, 885
Rowan-Robinson M. et al., 1991, Nat, 351, 719
Rowan-Robinson M., Benn C. R., Lawrence A., McMahon R. G., Broadhurst T. J., 1993, MNRAS, 263, 123
Sanders D. B., 1992, ASP Conf. Ser. Vol. 31. Astron. Soc. Pac., San Francisco, p. 303
Sanders D. B., Mirabel I. F., 1996, ARA&A, 34, 749
Sanders D. B., Soifer B. T., Elias J. H., Neugebauer G., Matthews K., 1988, ApJ, 328L, 35
Schmidt M., Green R. F., 1983, ApJ, 269, 352
Serjeant S., Lacy M., Rawlings S., King L. J., Clements D. L., 1995, MNRAS, 276L, 31
Siebenmorgen R., Kruegel E., 1992, A&A, 259, 614
Soifer B. T. et al., 1984, ApJ, 278L, 71
Soifer B. T., Neugebauer G., Matthews K., Armus L., 1994, ApJ, 433L, 69
Solomon P. M., Downes D., Radford S. J. E., 1992, ApJ, 398L, 29
Surace J. A., Sanders D. B., Vacca W. D., Veilleux S., Mazzarella J. M., 1998, ApJ, 492, 116
Taniguchi Y., Ikeuchi S., Shioya Y., 1999, ApJ, 514L, 9
Tripp T. M., Bechtold J., Green R. F., 1994, ApJ, 433, 533
Urry C. M., Falomo R., Scarpa R., Pesce J. E., Treves A., Giavalisco M., 1999, ApJ, 512, 88
Verma A., Rowan-Robinson M., McMahon R., Efstathiou A., 2001, MNRAS, submitted
Wilman R. J., Fabian A. C., Cutri R. M., Crawford C. S., Brandt W. N., 1998, MNRAS, 300L, 7
Yun M. S., Scoville N. Z., 1998, ApJ, 507, 774

This paper has been typeset from a TEX/LATEX file prepared by the author.

© Royal Astronomical Society • Provided by the NASA Astrophysics Data System